

**DETERMINATION OF MATERIAL PROPERTIES IN STRUCTURAL
SEALANT GLAZING APPLICATIONS**

**BESTIMMUNG VON MATERIALEIGENSCHAFTEN IN STRUCTURAL
SEALANT GLAZING ANWENDUNGEN**

**DETERMINATION DES PROPRIETES DES MATERIAUX UTILISEES PAR
VITRAGES EXTERIEURS COLLES**

Gunter Krüger and Hongguo Zhu

Summary

The silicone used in structural sealant glazing applications shows a characteristic rubber like behaviour. Standardized test specimens are used for the determination of material properties. However the results cannot be applied to other joint dimensions due to the complex stress distribution induced by the joint geometry. This is showed by means of finite element calculations for tension and shear tests. The material parameters of the silicone were determined by comparison of the test results and results of the calculations.

Zusammenfassung

Die bei Structural Glazing eingesetzten Silikonkleber zeigen ein charakteristisches gummielastisches Verhalten. Zur Bestimmung von Materialeigenschaften werden Versuche mit standardisierten Probekörpern durchgeführt. Die Ergebnisse können aber nicht ohne weiteres auf andere Klebefugenabmessungen übertragen werden, da im Probekörper ein komplexer Spannungszustand induziert wird. Dies wird mit Hilfe von Finite Elemente Berechnungen für den Zugversuch und den Scherversuch aufgezeigt. Durch Vergleich von Versuchs- und Rechenergebnissen werden die Materialparameter des Silikonklebers bestimmt.

Résumé

La silicone utilisée dans les vitrages extérieurs collés montre un comportement élastique caractéristique pour un caoutchouc. Pour déterminer les propriétés de matériau on a réalisé des essais avec des éprouvettes standardisées. Pourtant les résultats ne peuvent pas être appliqués à d'autres dimensions de joint étant donné la distribution de contraintes induites par la géométrie du joint. Ceci est montré par des calculs d'éléments finis pour l'essai de traction et l'essai de cisaillement. Par comparaison des résultats d'essai et de calcul les paramètres de matériau de la silicone sont déterminés.

Key Words

Structural Sealant Glazing, Silicone Rubber,
Finite Elasticity, Mooney-Rivlin Parameters

1. Introduction

As a method to attach panels of glass or other materials to the curtain wall of a building, structural sealant glazing has become of increasing importance [1],[2]. For this application silicone sealants are the only material that have suitable properties with regard to elasticity, adhesion and durability [3]. Nowadays there is a trend to use structural sealant glazing systems without an additional mechanical safety precaution. Therefore a particular attention has to be payed on the design and the bearing capacity of the sealant joints.

Standard tests for the determination of the material parameters, adhesion and the ultimate properties of the silicone make use of test specimens that are similar in geometry to the joints of real structural glazing elements [4]. This is useful to estimate the performance of practical joint designs. But these tests do not enable the material parameters to be deduced directly due to the complex stress distribution in the sealant induced by the joint geometry. They cannot be applied to other load cases [5] and other joint dimensions.

2. Silicone Rubber, General Properties

Silicone rubber is a macromolecular polymer composed from -Si-O- radicals and organic side groups that are attached to the silicone atoms [6],[7]. The mechanical properties of the silicone are characteristic of rubber like elastomers. In particular, silicone is approximately incompressible and sustains large elastic deformations prior fracture in conjunction with a distinctive nonlinear stress-strain characteristic as shown exemplary in fig.2.1. Furtheron a dependence on deformation history and time dependent effects (relaxation, creep) are observed. In comparison to other rubber like materials the elastic properties vary only slightly with temperature and silicon rubber can be used over a wide temperature range [3].

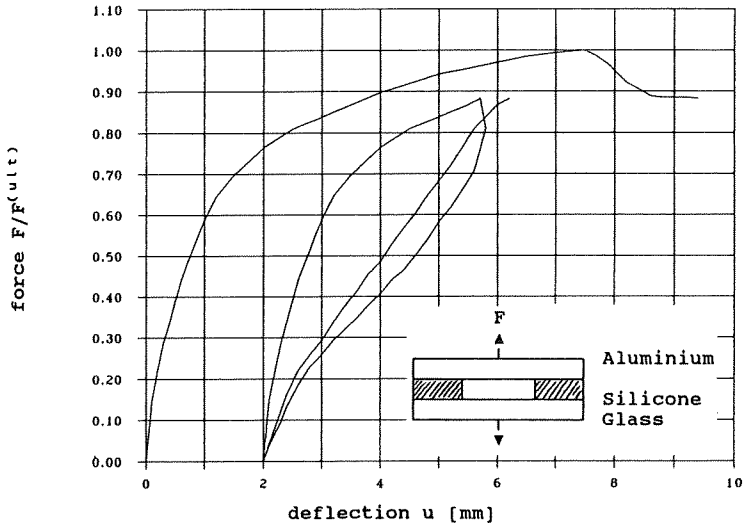


Fig.2.1 tension test,
nonlinear stress-strain-characteristic,
dependence on deformation history

3. Determination of Material Parameters

3.1 Theory

Since silicone is elastic up to strains of about hundred percent, the assumptions of infinitesimal elasticity are invalid. The macroscopic description of the mechanical behaviour has to consider finite deformations. Neglecting time dependence and effects that cause energy dissipation the constitutive equation of an isotropic elastic material is derived from the strain energy W as a function of the strain tensor invariants I_1, I_2, I_3 that are given in principal axis by the equations 3.1a-c.

$$I_1 = \alpha_1^2 + \alpha_2^2 + \alpha_3^2 \quad (3.1a)$$

$$I_2 = \alpha_1^2 \cdot \alpha_2^2 + \alpha_2^2 \cdot \alpha_3^2 + \alpha_3^2 \cdot \alpha_1^2 \quad (3.1b)$$

$$I_3 = \alpha_1^2 \cdot \alpha_2^2 \cdot \alpha_3^2 \quad (3.1c)$$

The principal stretch ratios α_i are related to the engineering strains ϵ_i by

$$\alpha_i = 1 + \epsilon_i \quad (i=1,2,3) \quad (3.2)$$

and give the extended length $l_i = l_0 + u_i$ in the principal directions of an elementary cube divided by the original length l_0 in the undeformed configuration.

The strain energy W was formulated for natural rubbers by Mooney as a linear function of I_1 and I_2 , with $I_3=1$:

$$W = A \cdot (I_1 - 3) + B \cdot (I_2 - 3) \quad (3.3)$$

This formulation gives a good and simple model to describe the elastic behaviour of incompressible rubber like materials [8],[9],[10]. The Mooney-Rivlin constants $A = \delta W / \delta I_1$ and $B = \delta W / \delta I_2$ are obtained by differentiation and represent material parameters. Using the relation

$$E = 2 \cdot (1 + \mu) \cdot G = 3G \quad (3.4)$$

and a Poisson ratio $\mu=0.5$ for an incompressible material, the Young's modulus E and the shear modulus G are given in the limit of small strains by the sum of the Mooney-Rivlin constants.

$$E/3 = G = 2 \cdot (A + B) \quad (3.5)$$

The Mooney-Rivlin constants can be determined from a simple uniaxial tension test (fig.3.1), where a homogeneous stress field is produced. Introducing the condition of incompressibility (equation 3.6a) the principal stretch ratios α_i are given by the equations 3.6b-c [10].

$$I_3 = \alpha_1 \cdot \alpha_2 \cdot \alpha_3 = 1 \quad (3.6a)$$

$$\alpha_1 = \alpha \quad (3.6b)$$

$$\alpha_2 = \alpha_3 = \alpha^{-1/2} \quad (3.6c)$$

The nominal stresses $\sigma_i = F_i / A_0$ that are referred to the cross

section in the undeformed configuration A_0 are derived from the strain energy function by differentiation.

$$\sigma_i = \delta W / \delta \alpha_i \quad (3.7)$$

Using the equations 3.6a-c and 3.7 for the uniaxial tension test the force F per unit unstrained cross section A_0 becomes

$$F/A_0 = 2 \cdot (A + B \cdot \alpha^{-1}) \cdot (\alpha - \alpha^{-2}) \quad (3.8)$$

Fig.3.2 shows a force-deflection-curve typical of a rubber like elastomer that was obtained from a tension test using a dumbbell test specimen according to ASTM D412-80. The increase of force at large strains prior rupture can be attributed to stress induced cristallisation [9],[12]. This effect was not observed in the tests that are described in chapter 3 (see fig.2.1) using the silicone DC983 produced by Dow Corning.

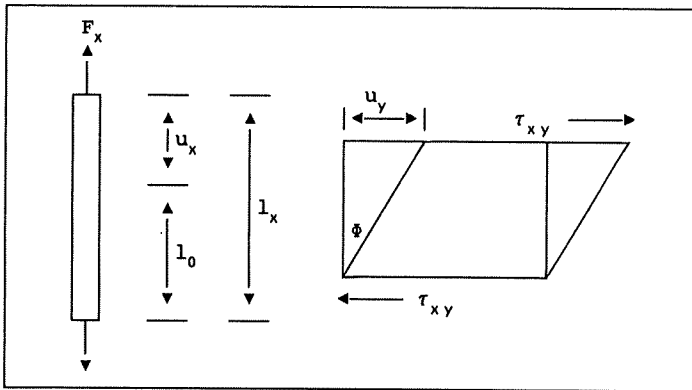


Fig.3.1 uniaxial tension, simple shear

To determine the MOONEY-RIVLIN constants A and B the force $F^* = (F/2A_0) \cdot (\alpha - \alpha^{-2})^{-1}$ is plotted versus α^{-1} (MOONEY plot, fig.3.3). The parameter B is represented by the slope and A is given by the intersection of the straight line with the F^* -axis. The Mooney-Rivlin approximation according to the straight line in fig.3.3 fits the experimental curve well for stretch ratios

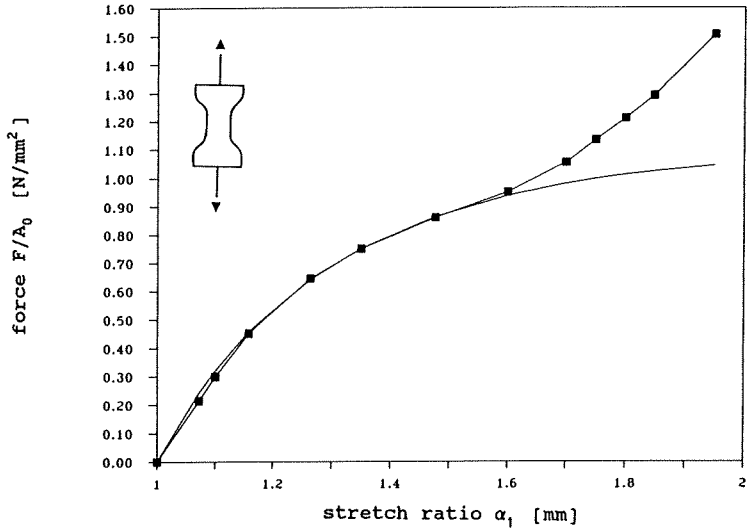


Fig.3.2 tension test using a dumbbell test specimen

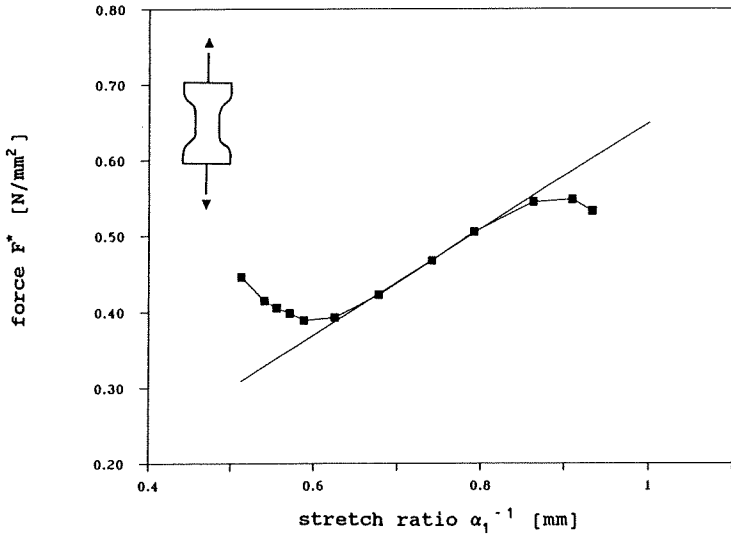


Fig.3.3 Mooney plot

between 1.2 and 1.5 (fig.3.2). However, a parameter set with increased B and A+B=constant would give a better approximation for small stretch ratios.

Simple shear represents a laminar deformation parallel to a stationary plane (fig.3.1). The amount of shear Γ is given by the tangent of the shear angle ϕ . By definition simple shear is a deformation where the volume remains constant independent of the Poisson ratio. The principal stretch ratios α_i are [11]

$$\alpha_1 = \alpha \quad (3.9a)$$

$$\alpha_2 = \alpha^{-1} \quad (3.9b)$$

$$\alpha_3 = 1 \quad (3.9c)$$

The strain energy function W (equation 3.4) becomes

$$\begin{aligned} W &= (A + B) \cdot (\alpha^2 + \alpha^{-2} - 2) \quad (3.10a) \\ &= (A + B) \cdot (\alpha - 1/\alpha)^2 \end{aligned}$$

and with $\Gamma = \alpha - 1/\alpha$ [11]

$$W = (A + B) \cdot \Gamma^2 \quad (3.10b)$$

It follows from equation 3.7, that the shear stress τ is a linear function of the shear Γ .

$$\tau = \delta W / \delta \Gamma = 2 \cdot (A + B) \cdot \Gamma = G \cdot \Gamma \quad (3.11)$$

3.2 Tests

The specimens used for tension and shear tests are shown in Fig.3.4. The test specimen is symmetrical with two sealant joints of 20mm width, 10mm thickness and 50mm length. The silicone was DC983. Tension and shear forces were applied at the glass plate. During the tests the external force and the deflection were measured. The extension rate was 5mm/s.

The standardized ISO/DIS 9047 and DIN 52455 test specimens shown in fig.3.4 are currently used to determine the material properties of the silicone, rupture values and the resistance of the joint to shear and tensile forces. The test joint has a

width of $b_j = 12\text{mm}$ ('bite') and a thickness of $h_j = 12\text{mm}$. The joint length is 50mm. The substrates are the materials (glass, aluminium, etc.) used in the structural glazing unit.

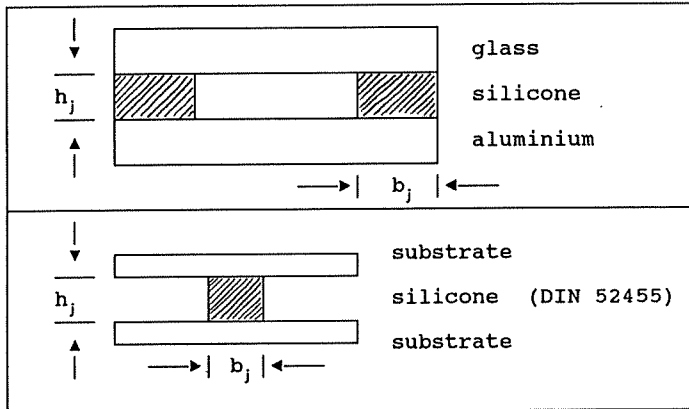


Fig.3.4 test specimen

Using this kind of specimens in uniaxial tension tests, it is obvious, as it follows from the incompressibility of the silicone, that the lateral contraction leads to stresses at the constrained boundary of the silicone and the stress field is not homogeneous. Consequently the slope of the load-deformation curves at small strains (tangent modulus E_t) is geometry dependent and may differ considerably from the material parameter Young's modulus E . The results cannot be applied to other sealant dimensions. On the contrary, the center zone of a dumbbell test specimen, according to ASTM D 412-80, is approximately not affected by boundary layer stresses and therefore can be used for the direct measurement of the linear and nonlinear material parameters.

Simple shear is produced by a laminar deformation parallel to a stationary plane. The tangent modulus G_t is equal to the material parameter G . Within the limit of small strains there are no lateral effects. However, in the shear tests a tangen-

tial force was applied at the glass plate that does not exactly lead to a simple shear deformation due to the force balance. An approximately homogeneous stress field is produced only in the center zone of the test volume. To reduce boundary effects at the corners of the test volume, the test specimen should be long and flat.

3.3 Finite Element Analysis

The calculations were carried out using the ANSYS-PC 4.4A finite element program. The finite element model and the boundary conditions used for the analysis of the tension and shear tests are shown in fig.3.5 and fig.3.6. Because of symmetry only one sealant joint of the test specimen has to be modeled.

To describe the elastic properties of silicone at small strains a linear constitutive equation with the material parameters E and μ is appropriate. The silicone is assumed to be approximately incompressible and the Poisson ratio was set to 0.49. The input of $\mu=0.5$ would lead to a singularity because the stress field for the deformation of an incompressible material is undetermined to the amount of an arbitrary hydrostatic pressure.

Analyzing the tension test, the Young's modulus was determined by the value that gives for $\mu=0.49$ the best correspondence with the experimental tangent modulus E_t at small strains. In particular for Poisson ratios close to 0.5 the stiffness is considerably affected by the finite element size. To reduce discretisation errors a fine finite element mesh with 1mm lateral mesh size was used. The mesh size longitudinal to the sealant joint was 10mm.

In fig.3.7 the calculated modulus is given in dependence of the lateral size. With decreasing mesh size the calculated modulus converges to E that represents the material parameter of the silicone.

For problems involving large strains the Mooney-Rivlin constitutive law is available in ANSYS. The implementation of the

Mooney-Rivlin constitutive equation makes use of two additional terms in the strain energy function that depend on I_3 and consequently on the volumetric work [13].

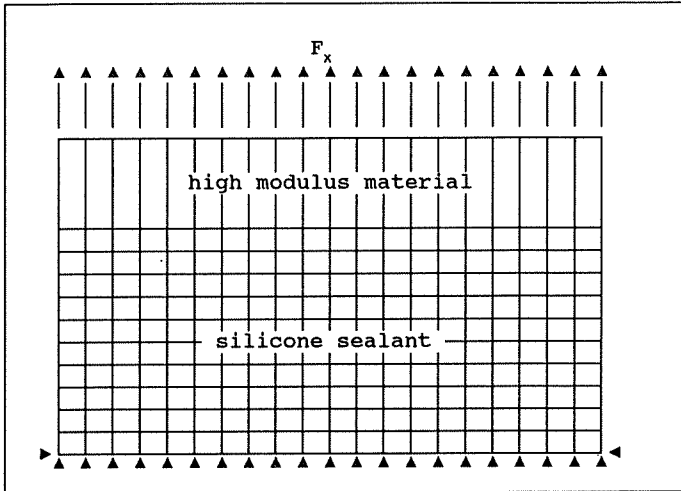


Fig.3.5 Finite element model, tension test

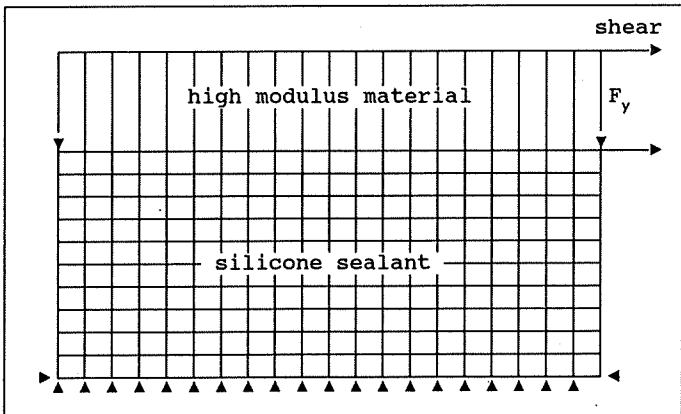


Fig.3.6 Finite element model, shear test

According to equation 3.4 the sum of the Mooney-Rivlin constants is proportional to the Young's modulus. The remaining free parameter was used to achieve a good fit to the experimental load-deflection curve in tension.

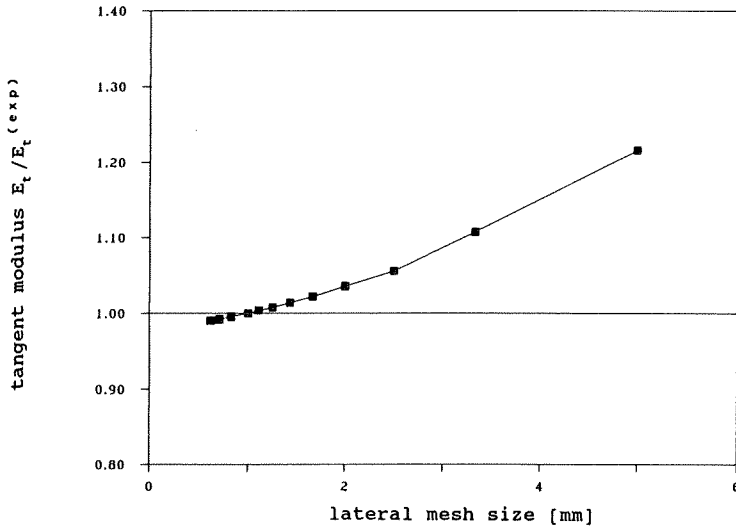


Fig.3.7 calculated modulus in dependence of the lateral mesh size

3.4 Results

The test results in tension and shear are given in the diagrams fig.3.8 and fig.3.9. The nominal stresses referred to the unstressed cross section $\sigma_x = F_x / A_0$ and $\tau_{xy} = F_y / A_0$ are plotted versus the engineering strain $\epsilon = u_x / h_j$ and the shear $\Gamma = u_y / h_j$, respectively. Further the experimental secant moduli $E_s^{(exp)} = \sigma(\epsilon) / \epsilon$ and $G_s^{(exp)} = \tau(\Gamma) / \Gamma$ are given as a function of the strain and the shear.

It can be seen that the load deformation curve in tension is highly nonlinear and that consequently the experimental secant modulus varies considerably with the strain. The tangent modu-

lus $E_t^{(exp)}$ at small strains is

$$E_t^{(exp)} = E_s^{(exp)} \Big|_{\epsilon=0} = 5N/mm^2 = E_t^{(FE)}$$

The Young's modulus $E=6(A+B)$ was found by means of finite element calculation with the condition $E_t^{(FE)}=E_t^{(exp)}$.

$$E = 6 \cdot (A + B) = 2.13N/mm^2$$

Fitting the calculated to the measured load-deflection curve in tension with the condition $6(A+B)=2.13N/mm^2$ the Mooney-Rivlin parameters were determined to

$$A = 0.055N/mm^2 \quad \text{and} \quad B = 0.30N/mm^2$$

In contrast to the tension test, the stress-strain curve in shear is almost linear in Γ . The experimental tangent modulus $G_t^{(exp)}$ at small shear is

$$G_t^{(exp)} = G_s^{(exp)} \Big|_{\Gamma=0} \approx 0.78N/mm^2$$

and differs about 15% from the tangent shear modulus

$$G_t^{(FE)} = 0.66N/mm^2$$

found by means of finite element calculation with $\mu=0.49$. From equation 3.4 the shear modulus is calculated to

$$G = E/2 \cdot (1+\mu)^{-1} = 0.71N/mm^2$$

Differences between the experimental and calculated tangent shear moduli may be assigned to inadequacies in the boundary conditions of finite element model.

The calculated nominal stress-strain curves (∇) and the calculated secant moduli (\blacktriangle) are given in fig.3.8 and fig.3.9. Stress contour plots are shown in the fig.3.10 for tension and in fig.3.11 for shear. The stresses S_x and S_{xy} are true Cauchy stresses that are related to the deformed cross

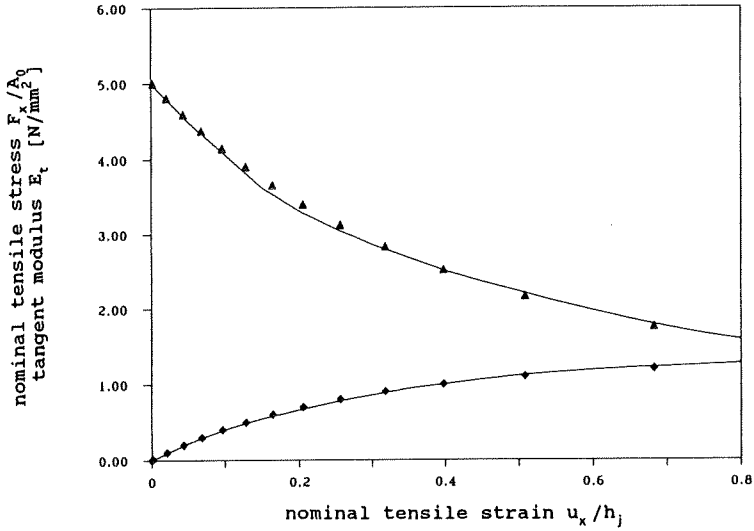


Fig.3.8 tension test, measured (-) and calculated (◆,▲) nominal stress-strain curves and secant moduli

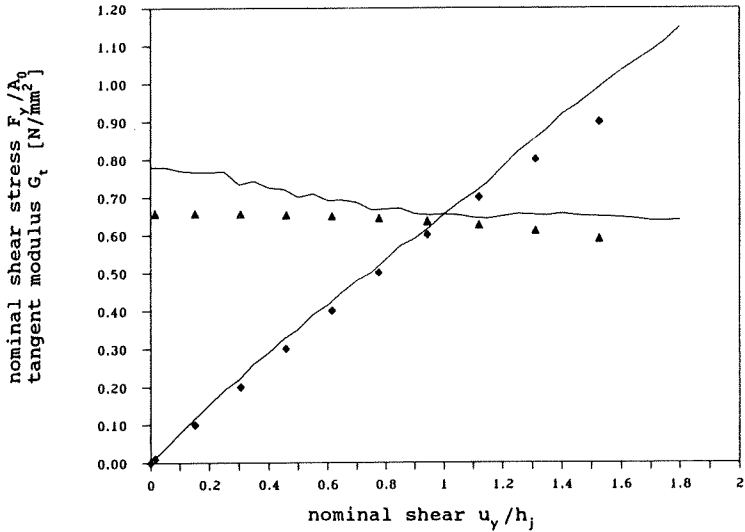


Fig.3.9 shear test, measured (-) and calculated (◆,▲) nominal stress-strain curves and secant moduli

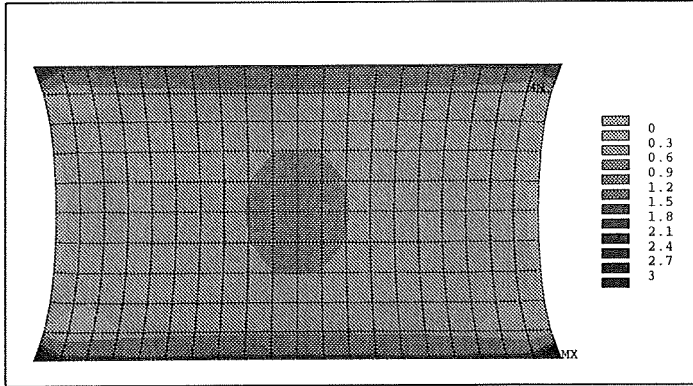


Fig.3.10 stress S_x contour plot, deformed structure
(tension, $F_x/A_0=0.5N/mm^2$)

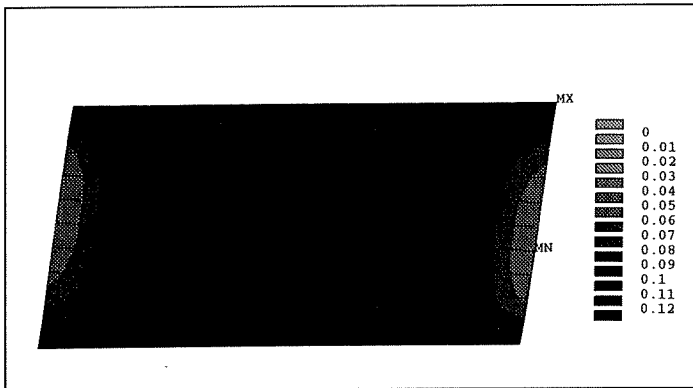


Fig.3.11 stress S_{xy} contour plot, deformed structure
(shear, $F_y/A_0=0.1N/mm^2$)

4. Variation of the Joint Dimensions

Using the linear constitutive equation the variation of the tangent modulus (resistance to tension and shear forces) was calculated in the limit of small strains. The bite was varied between 10mm and 24mm and the joint thickness was varied between 5mm and 12mm. The results are given in the tables 4.1

and 4.2 for tension and shear and are illustrated in fig.4.1 and fig.4.2. The tangent moduli E_t and G_t are plotted as a function of the bite b_j . The results were divided by $5N/mm^2$ for tension and by $0.78N/mm^2$ for shear, respectively.

h_j	b_j							
	10	12	14	16	18	20	22	24
5	5.56	6.48	7.35	8.24	9.12	10.0	10.8	11.6
6	4.90	5.49	6.12	6.80	7.48	8.16	8.84	9.48
7	4.43	4.87	5.35	5.86	6.39	6.94	7.48	8.01
8	4.12	4.45	4.82	5.23	5.65	6.08	6.52	6.96
9	3.90	4.16	4.45	4.77	5.11	5.46	5.82	6.18
10	3.73	3.94	4.18	4.44	4.71	5.00	5.30	5.60
11	3.60	3.78	3.97	4.18	4.41	4.65	4.90	5.15
12	3.50	3.65	3.81	3.98	4.17	4.37	4.58	4.80

table 4.1 resistance to tension forces

h_j	b_j							
	10	12	14	16	18	20	22	24
5	0.71	0.73	0.73	0.74	0.75	0.75	0.75	0.76
6	0.69	0.71	0.72	0.73	0.73	0.74	0.74	0.75
7	0.67	0.69	0.71	0.72	0.72	0.73	0.74	0.74
8	0.65	0.68	0.69	0.70	0.71	0.72	0.73	0.73
9	0.63	0.66	0.68	0.69	0.70	0.71	0.72	0.72
10	0.61	0.64	0.66	0.68	0.69	0.70	0.71	0.71
11	0.59	0.62	0.65	0.67	0.67	0.69	0.70	0.71
12	0.56	0.60	0.63	0.65	0.67	0.68	0.69	0.70

table 4.2 resistance to shear forces

and fig.4.2. The tangent moduli E_t and G_t are plotted as a function of the bite b_j . The results were divided by $5N/mm^2$ for tension and by $0.78N/mm^2$ for shear, respectively.

h_j	b_j							
	10	12	14	16	18	20	22	24
5	5.56	6.48	7.35	8.24	9.12	10.0	10.8	11.6
6	4.90	5.49	6.12	6.80	7.48	8.16	8.84	9.48
7	4.43	4.87	5.35	5.86	6.39	6.94	7.48	8.01
8	4.12	4.45	4.82	5.23	5.65	6.08	6.52	6.96
9	3.90	4.16	4.45	4.77	5.11	5.46	5.82	6.18
10	3.73	3.94	4.18	4.44	4.71	5.00	5.30	5.60
11	3.60	3.78	3.97	4.18	4.41	4.65	4.90	5.15
12	3.50	3.65	3.81	3.98	4.17	4.37	4.58	4.80

table 4.1 resistance to tension forces

h_j	b_j							
	10	12	14	16	18	20	22	24
5	0.71	0.73	0.73	0.74	0.75	0.75	0.75	0.76
6	0.69	0.71	0.72	0.73	0.73	0.74	0.74	0.75
7	0.67	0.69	0.71	0.72	0.72	0.73	0.74	0.74
8	0.65	0.68	0.69	0.70	0.71	0.72	0.73	0.73
9	0.63	0.66	0.68	0.69	0.70	0.71	0.72	0.72
10	0.61	0.64	0.66	0.68	0.69	0.70	0.71	0.71
11	0.59	0.62	0.65	0.67	0.67	0.69	0.70	0.71
12	0.56	0.60	0.63	0.65	0.67	0.68	0.69	0.70

table 4.2 resistance to shear forces

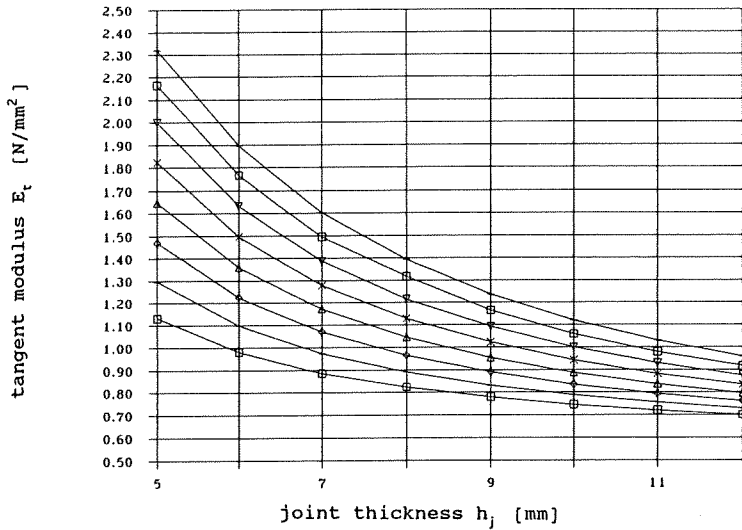


Fig.4.1 tangent modulus E_t as function of the joint dimensions b_j and h_j

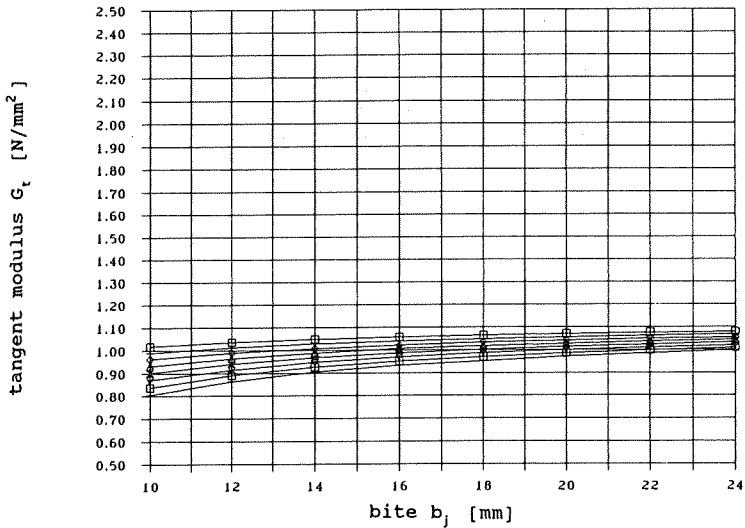


Fig.4.2 tangent modulus G_t as function of the joint dimensions b_j and h_j

The resistance to tension forces is approximately a linear function of the bite and decreases with increasing joint thickness as shown in the diagram. For very small b_j/h_j ratios the E_t gets close to the Young's modulus E .

In contrast to this, the resistance to shear forces is approximately a linear function of the joint thickness and increases with increasing bite. For very large b_j/h_j ratios the G_t gets close to the shear modulus G .

5. Conclusion

It has been shown that the Mooney-Rivlin constitutive equation is appropriate for the description of the mechanical behaviour of silicone in tension and shear. Test specimens that are similar in geometry to the sealant joint of structural glazing elements can be used to test the adhesion, the resistance to tension and shear forces and the bearing capacity of the silicone. The Young's modulus cannot be deduced directly from the simple tension test due to the complex stress field induced by the joint geometry. Although simple shear is not practicable experimentally, the shear modulus can be determined approximately from shear test on condition that the joint thickness to bite ratio does not exceed 0.5. The Mooney-Rivlin parameters can be determined by comparison of the tension test results and finite element calculations.

6. References

- [1] IKER, J, NEMETH, C., WOLF, A.:
Structural-Glazing - Eine neue Technik für die
Ganzglasfassade, Teil 1;
Glasforum 37 (1987), pp.37-40
- [2] KLOSOWSKY, J.: Sealants in Construction; Verlag Marcel
Dekker, New York (1989)
- [3] Kunststoff Handbuch, Band XI; Ed. Vieweg, Reiher,
Scheurlen: Hanser Verlag München (1971)

- [4] GUTOWSKI, V.W.S., RUSSELL, L., CERRA, A.:
New tests for the adhesion of silicone sealants;
Construction and Building Materials (1993) Vol 7,1
- [5] SANDBERG, L.B., AHLBORN, T.M.:
Combined Stress Behavior of Structural Glazing Joints;
J.Struct.Engrg., ASCE 115(5) (1989), pp.1212-1224;
- [6] Kunststoff Handbuch Band I; Ed. Becker, Braun;
Hanser Verlag München (1990)
- [7] BRYDSON, J.A.: Rubberly Materials and their Compounds
Elsevier Applied Science, New York (1989)
- [8] RIVLIN, R.S.: Large Deformations;
Rheology, Theory and Applications, Vol.1 pp.361-385
Ed. Eirich, F.R.; Academic Press, New York (1956)
- [9] BLATZ, P.J.: Application of large deformation theory
to the thermomechanical behavior of rubberlike
polymers -porous, unfilled, and filled;
Rheology, Theory and Applications, Vol.5 pp.1-55
Ed. Eirich, F.R.; Academic Press, New York (1969)
- [10] DE BORST, R., VAN DEN BOGERT, P.A.J., ZEILMAKER, J:
Modelling and analysis of rubberlike materials;
Heron, Vol.33, No.1 (1988)
- [11] TRELOAR, L.R.G.: The Physics of Rubber Elasticity;
Oxford University Press, London (1958)
- [12] Polymere Werkstoffe Band I, Chemie und Physik;
Ed. Batzer, H.; Thieme Verlag Stuttgart (1985)
- [13] ANSYS User's Manual Rev.4.4 Vol. I and II